Large-Yield Preparation of High-Electronic-Quatity Graphene by a Langmuir-Schaefer Approach

Gengler, Regis Y. N.; Veligura, Alina; Enotiadis, Apostolos; Diamanti, Evmorfia K.; Gournis, Dimitrios; Jozsa, Csaba; van Wees, Bart J.; Rudolf, Petra

Published in:
Small

DOI:
10.1002/smll.200901120

Publication date:
2010

Submitted to small NANO MICRO

Supporting Information

I. Powder X-Ray Diffraction (XRD)

II. Differential thermal and thermogravimetric analysis (DTA-TG)

III. FTIR Spectroscopy

IV. Raman Spectroscopy

V. Electronic properties; as prepared vs mechanically exfoliated graphene

VI. Atomic force microscopy micrographs.

VII. Optical photography.

I. Powder X-ray Diffraction (XRD)

X-ray powder diffraction data were collected on a D8 Advance Bruker diffractometer by using CuKα (36 kV, 36 mA) radiation and a secondary beam graphite monochromator. The patterns were recorded in the 2-theta (2θ) range from 2º to 60º, in steps of 0.02º and counting time of 2s per step. The X-ray diffraction (XRD) patterns of the pristine graphite and graphene oxide are shown in Fig. S1. The pattern of pure graphite shows a peak at 26.6º corresponding to a basal spacing d_{002} = 3.34 Å. The pattern of graphene oxide, on the other hand, exhibits a 001 reflection [1,2] at 12.0º corresponding to a basal spacing of d_{001} = 7.33 Å.

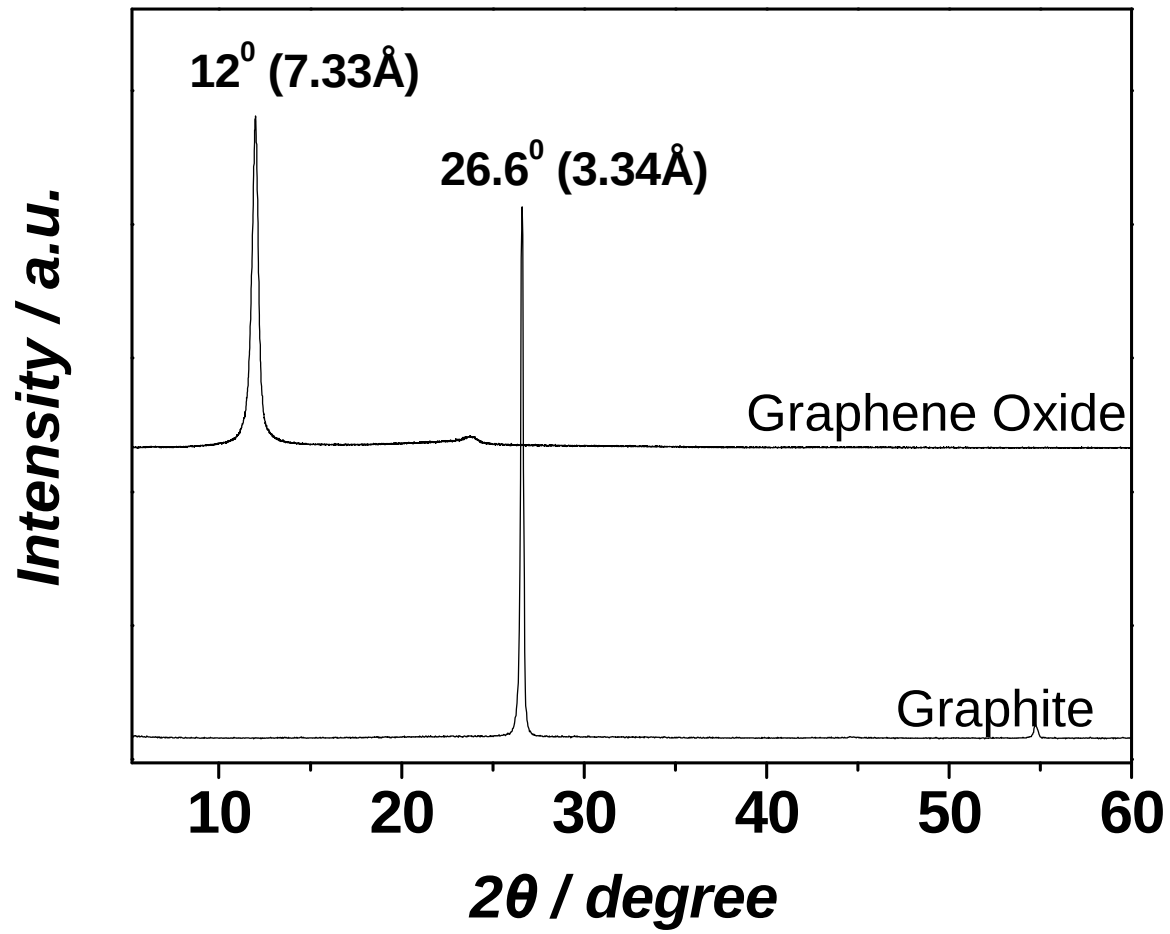

Figure S1

II. DTA-TG analysis

Thermogravimetric (TGA) and differential thermal (DTA) analysis were performed using a Perkin Elmer Pyris Diamond TG/DTA. Samples of approximately 5 mg were heated in air from 25 to 850 °C, at a rate of 5 °C/min. DTA curve of graphene oxide (Fig. S2) exhibits two exothermic peaks at 250°C and 500°C, which correspond to 30% and 50% weight losses, respectively. These peaks are attributed to the removal of oxygen containing groups (first peak) and to carbon combustion (second peak).[2] The DTA curve of graphite shows instead only one exothermic peak at 700 °C.

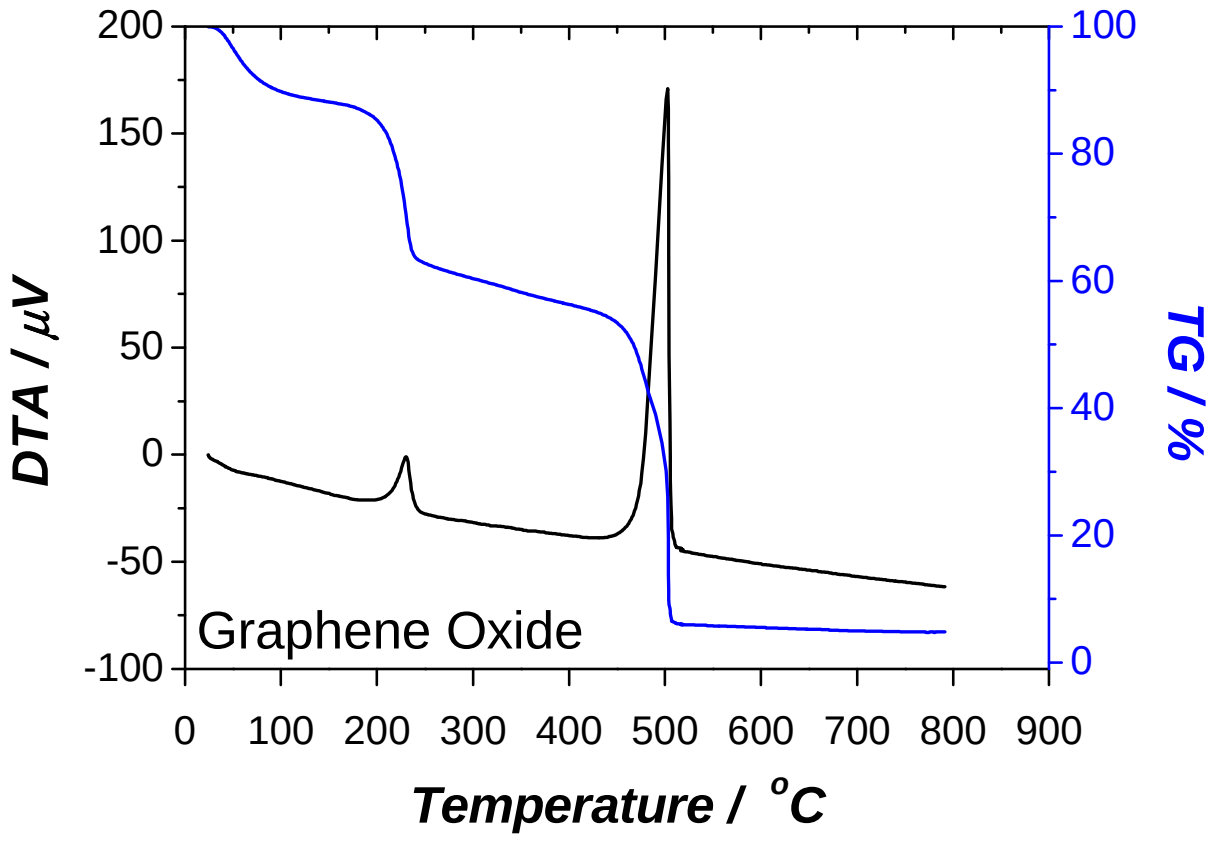

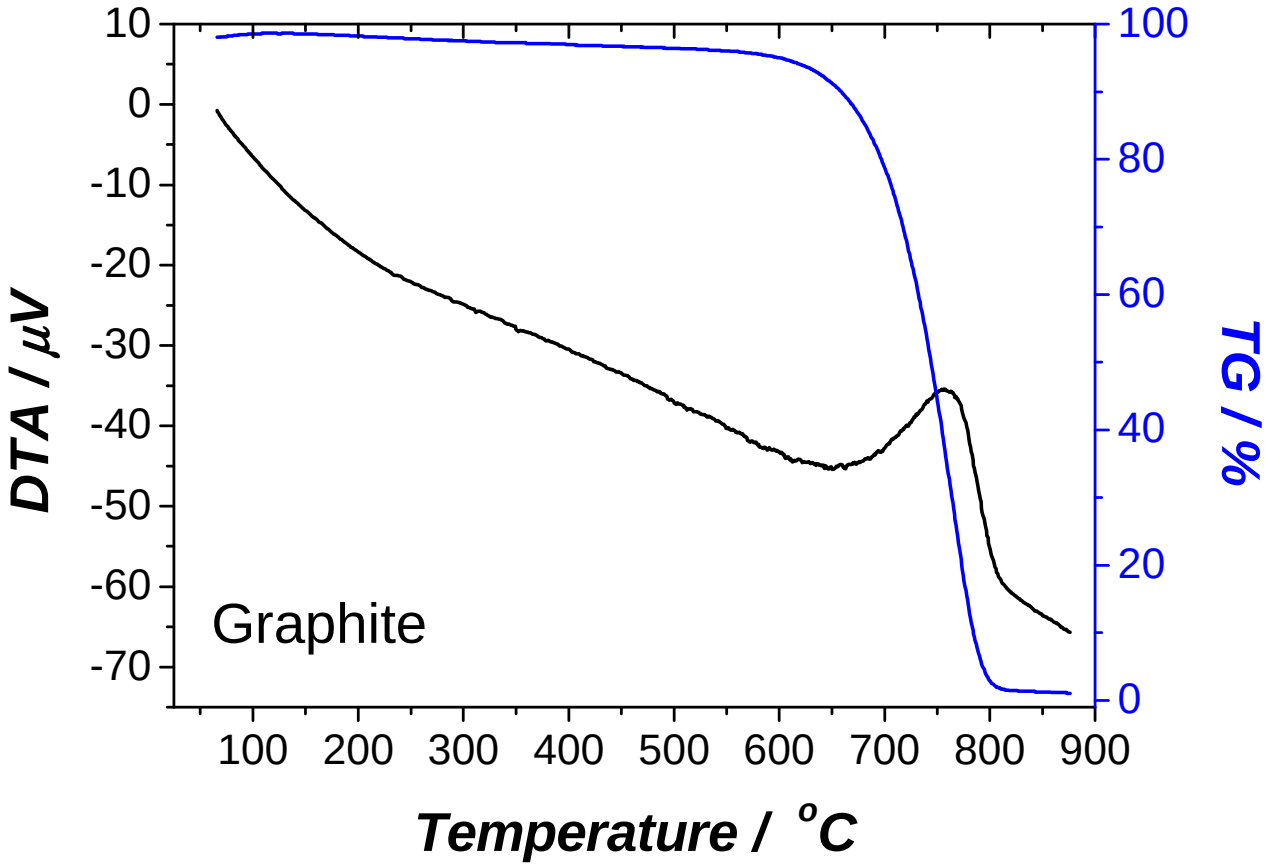

Figure S2

III. FTIR Spectroscopy

An additional tool for the characterisation of graphene oxide is FTIR spectroscopy. As shown in Fig. S3, graphene oxide exhibits the following characteristic IR features: a weak shoulder at 3410 cm^{-1} attributed to the hydroxyl stretching vibrations of the C-OH groups, a weak band at 1620 cm^{-1} assigned to the C=O stretching vibrations of the-COOH groups, a strong band at 1396cm^{-1} assigned to the O-H deformations of the C-OH groups, and a strong band at 1062 cm^{-1} attributed to C-O stretching vibrations.[2] Pur graphite is an IR inactive solid and its

spectrum does not show these bands. Infrared spectra were measured with a Shimadzu FT-IR 8400 spectrometer, in the region of 500-4000 cm^{-1} equipped with a deuterated triglycine sulfate (DTGS) detector. Each spectrum was the average of 120 scans collected at 2 cm^{-1} resolution. Samples were in the form of KBr pellets containing ca. 2 wt % sample.

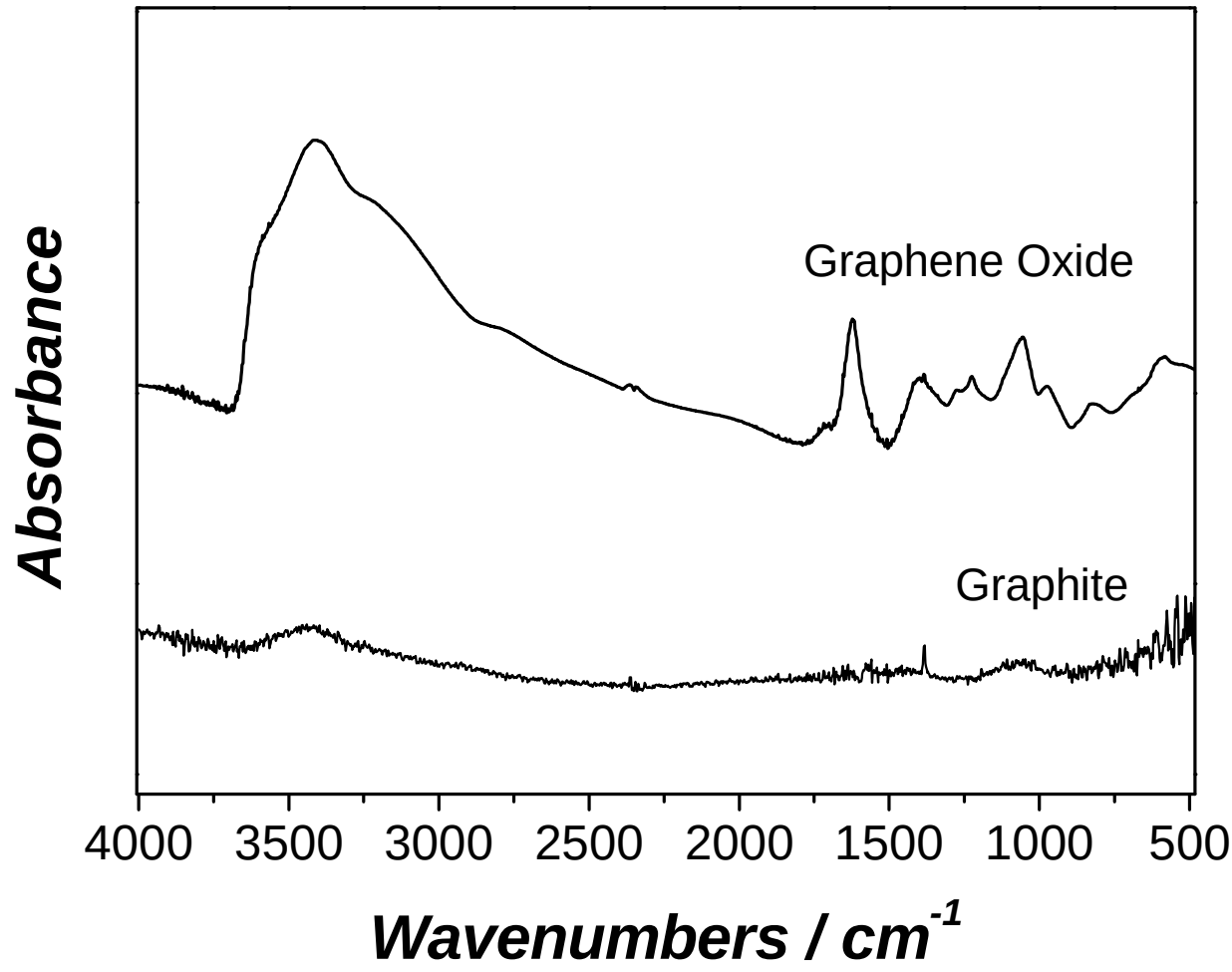

Figure S3.

IV. Raman Spectroscopy

Raman spectroscopy is a widely used tool for the characterization of carbon products. Raman spectra were recorded with a Micro – Raman system RM 1000 (RENISHAW) using a laser

excitation line at 532 nm (Nd – YAG) in the range of 1000 – 2400 cm^{-1}. A power of 1 mW was used with 1μm focus spot in order to avoid photodecomposition of the samples. The Raman spectrum (Fig. S4) of pristine graphite displays the prominent G band at 1580 cm^{-1} corresponding to the first-order scattering of tangential stretching (E_{2g}) mode, while the D band at 1353 cm^{-1} is very weak and originates from disorder in the sp^2–hybridized carbon atoms, characteristic for lattice distortions in the graphene sheets.[3] In the Raman spectrum of graphene oxide the G band is broadened and shifted to 1594 cm^{-1} whereas the D band at 1363 cm^{-1} becomes the prominent feature in the spectrum testifying to indicating the creation of sp^3 domains due to the extensive oxidation.[3] The intensity ratio of the D and G bands is a measure of the disorder, as expressed by the sp^2/sp^3 carbon ratio. Fig. S4 (B) shows the Raman spectra of GO sheets deposited by the LS method on gold substrates before and after reduction and annealing. After chemical reduction and annealing, the sheets show a noticeable decrease in the D/G ratio from 1.02 to 0.75. This observation suggests that while most of the oxygenated groups are removed (in the form of CO or CO_2), the relative amount of disordered sp^2-hybridized atoms is still high. The later could be explained either by the fact that amine molecules covalently bound to graphene survive the reduction and annealing procedures (contributing to an enhanced sp^3 hybridization) or that vacancies produced during production of GO remain unchanged by the reduction process and ultimately define the intact graphene regions.[4,5] Therefore, determining the degree of functionalization was not possible using Raman spectroscopy.

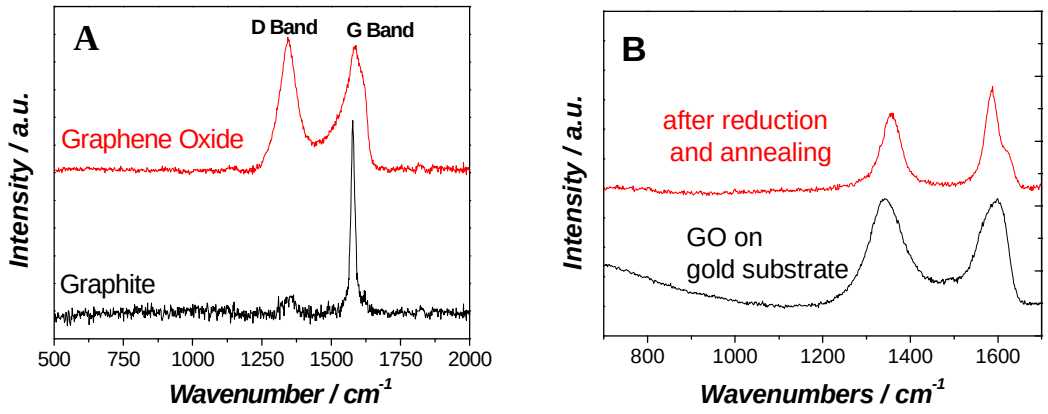

Figure S4.

V. Electronic properties; as prepared vs mechanically exfoliated graphene

Illustration of the scaling factors by overlapping the resistivity measurement of the GS as prepared by our approach (9 min. annealing) (red line; top and right scales) versus a typical curve obtained on mechanically cleaved graphene (black circles; bottom and left scales)(Fig. S5) .

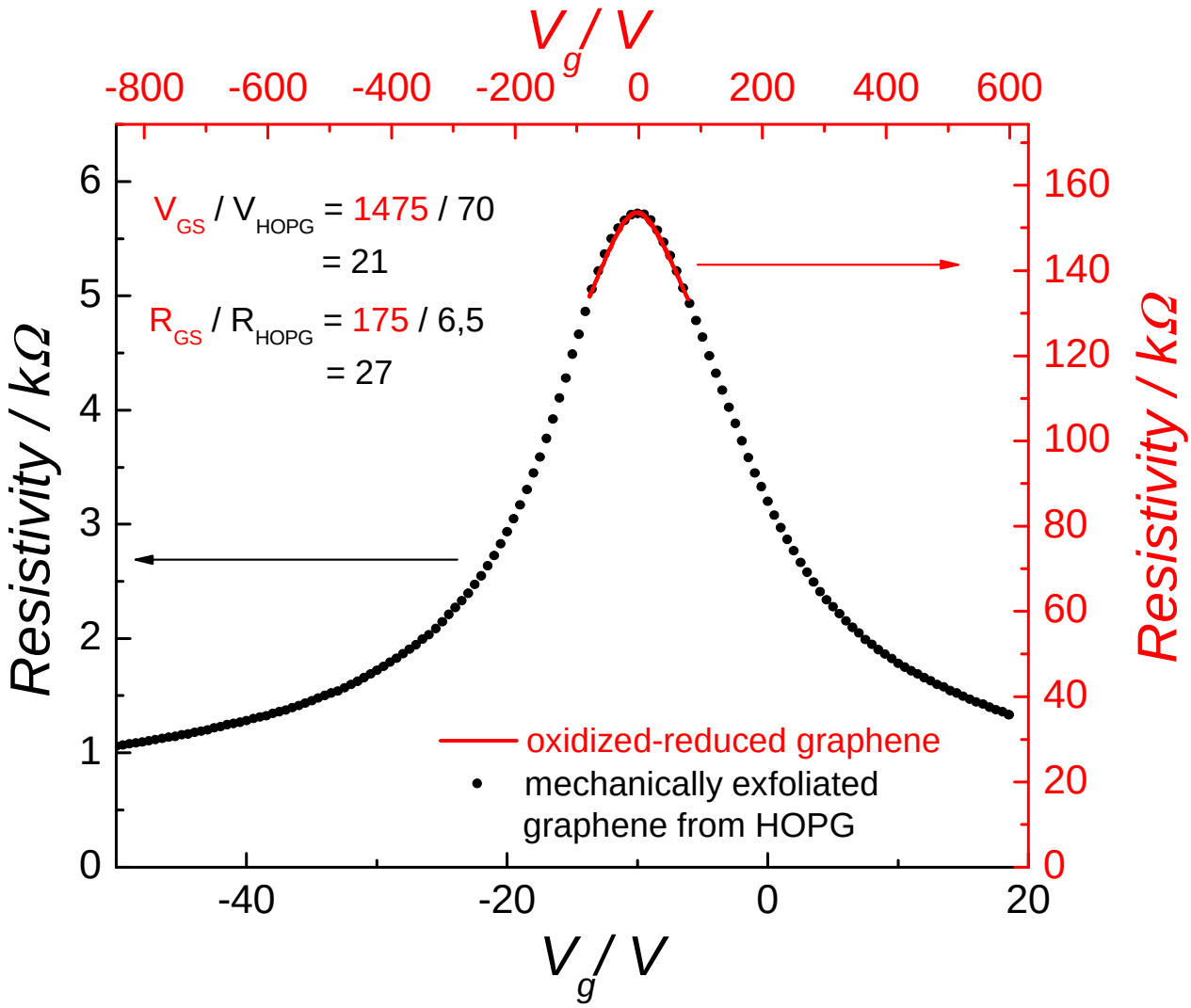

Figure S5

Sheet resistivity of GS (exposed to ethylene for 90 min) versus gate voltage (Fig. S6).

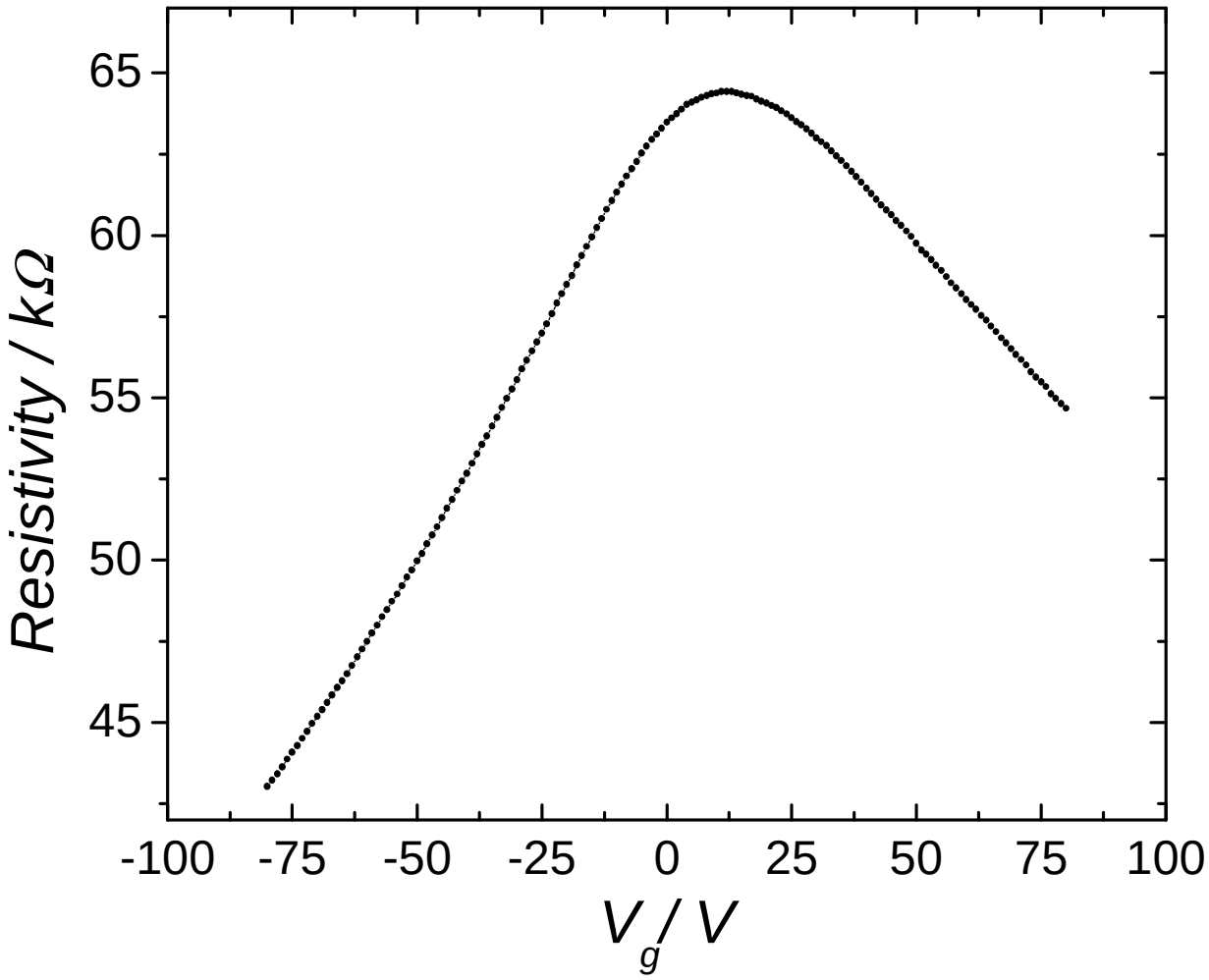

Figure S6

Illustration of the scaling factors by overlapping the resistivity measurement of the GS exposed to ethylene for 90 min. (red line; top and right scales) versus a typical curve obtained on mechanically cleaved graphene (black circles; bottom and left scales) (Fig. S7) .

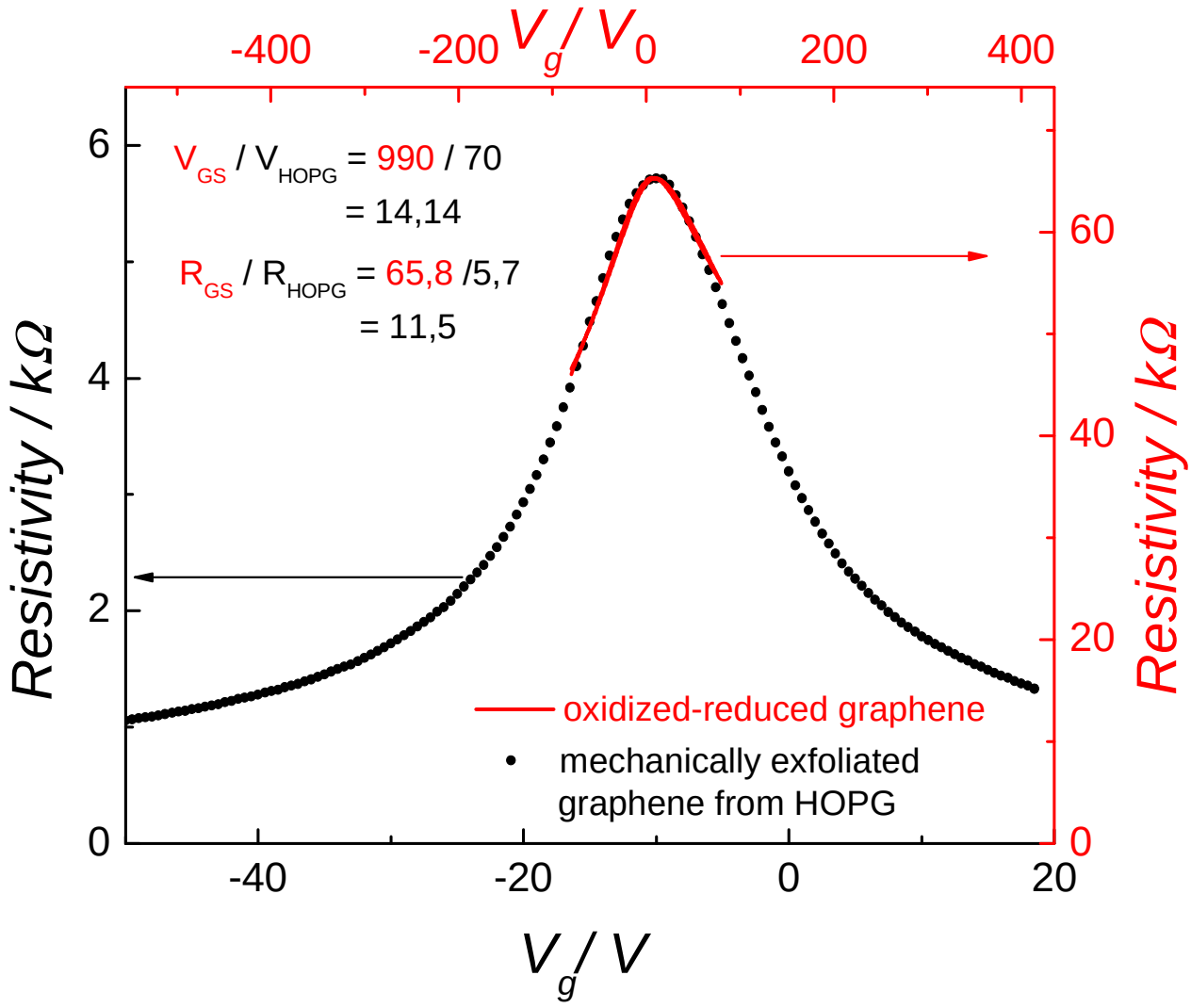

Figure S7

VI. Atomic force microscopy micrographs.

To prove the flexibility of the method regarding the type of substrate suitable, deposition were performed not only on Au (fig. S8D) but also on pure and HMDS treated SiO_2. HMDS treatment makes SiO_2 more hydrophobic. Silicon was chosen for simplicity since the possibility to localize the flakes by optical microscopy facilitates the AFM measurements and allows for an easy approach to the region of interest. To increase the chance of imaging graphene flakes on the gold substrate, we chose to deposit at a high ODA-GO surface pressure to obtain a high coverage. Examples of AFM micrographs of GO deposited on

HMDS-treated SiO_2 are displayed in figure S8 A and B; one can clearly observe the presence of the graphene oxide flakes. The white dots are assigned to the HMDS treatment. Figure S8 C shows GO deposited on untreated SiO_2; as in fig S8A,B, large graphene oxide flakes, like the ones imaged here, can easily be seen everywhere on the substrate surface. Finally, an AFM image of graphene oxide deposited on gold is shown in figure S8D; one can distinguish the graphene sheets against the darker background (gold surface). Due to the high ODA-GO surface pressure employed, a high coverage is observed and overlapping flakes appear white on the micrograph.

Measurment were performed using a AFM Nanoscope IV (Veeco) and Scientec 5100 (Scientec).

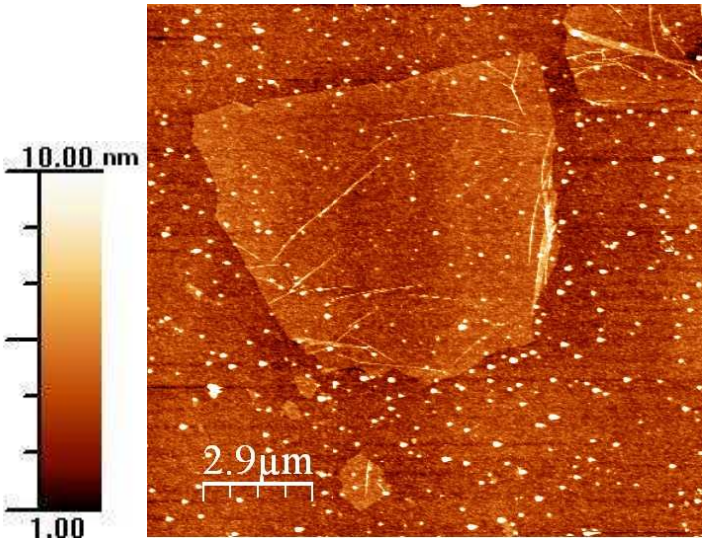

A) P=0.0mN, substrate HMDS/SiO_2

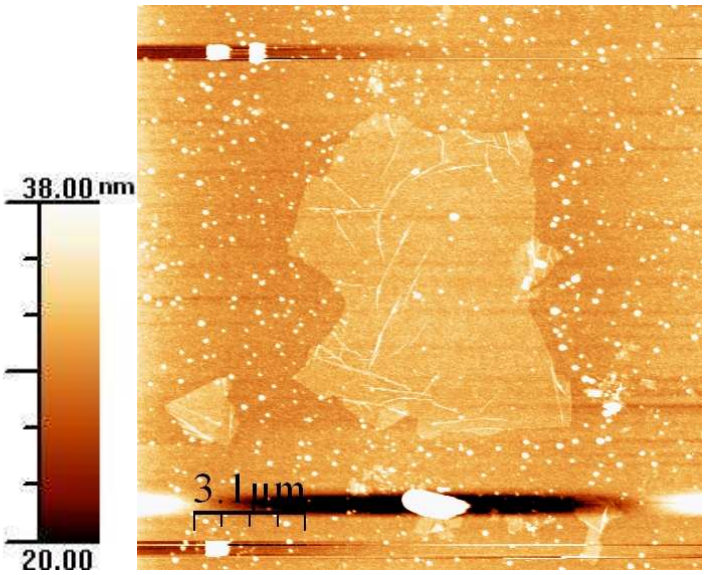

B) P=0.0mN, substrate HMDS/SiO_2 under a PMMA resist layer

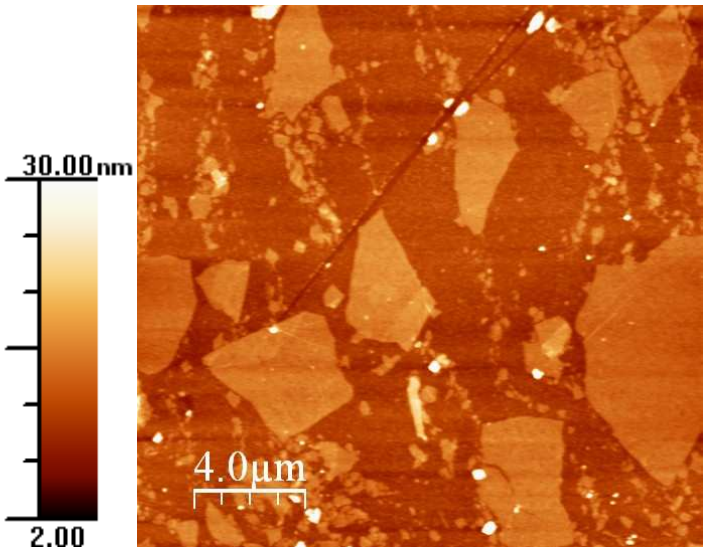

C) P=20.0mN, on substrate SiO_2 as received.

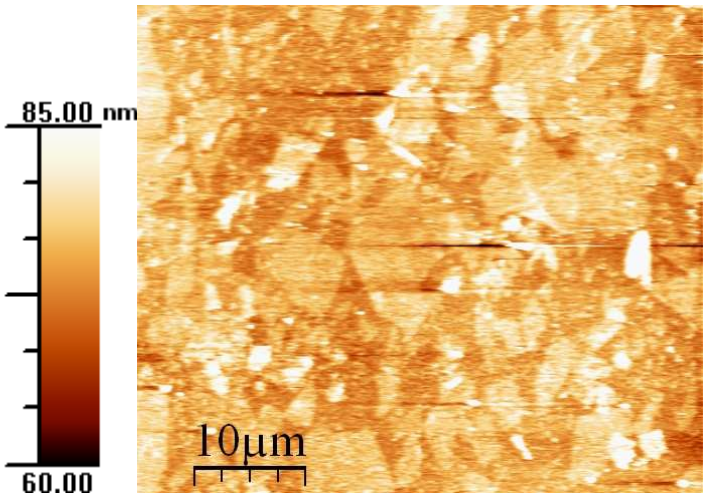

D) P=40.0mN, substrate gold on mica.

Figure S8

VII. Optical photography.

The photograph shown in figure S9 demonstrates that our approach can be extended to a larger scale, i.e. deposition on a full 3 inch Si wafer. On the right hand side one sees the as-received wafer with its SiO_2 surface layer, on the left hand side the wafer where the SiO_2 is covered by 1 layer of GO deposited by LS. Due to white light interference between the dielectric layer and the deposited film, one can observe a clear contrast between the purple-violet coloration of the SiO_2 layer and the green hue resulting from the deposited GO.

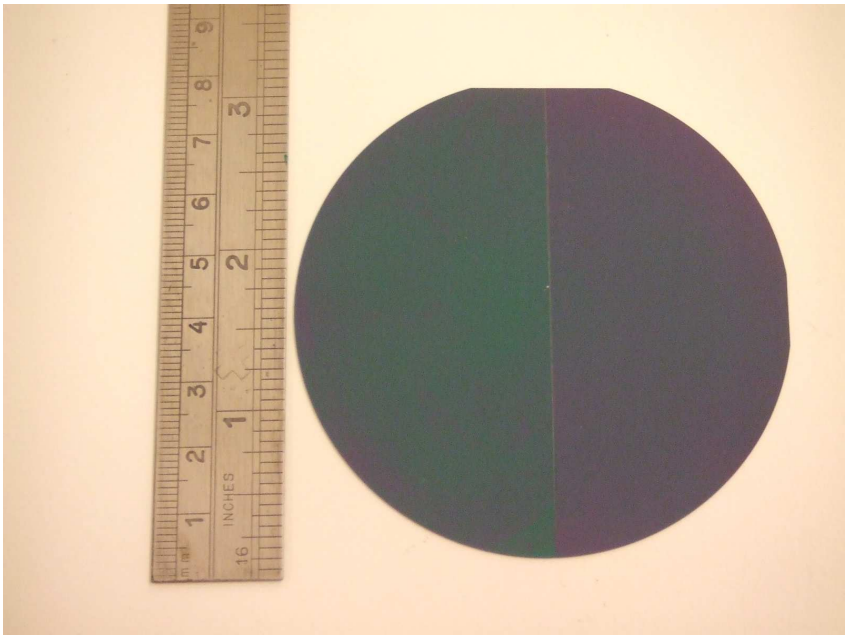

Figure S9

References

[1] C. Nethravathi, B.Viswanath, C. Shivakumara, N. Mahadevaiah, M. Rajamathi. *Carbon* **2008**, ***46***, 1773.

[2] A.B. Bourlinos, D. Gournis, D. Petridis, T. Szabo, A. Szeri, I. Dekany. *Langmuir* **2003**, *19*, 6050.

[3] S.Stankovich, D.A.Dikin, R.D.Piner, K.A. Kohlhaas, A. Kleinhammes, Y. Jia, Y.Wu, S.T.Nguyen, R. S. Ruoff. *Carbon* **2007**, *45***,** 1558.

[4] C. Gmez-Navarro, R.T. Weitz, A.M. Bittner, M. Scolari, A. Mews, M. Burghard, K. Kern. *Nano Letters* **2007**, *7*, 3499.

[5] J.R. Lomeda, C.D. Doyle, D.V. Kosynkin, W-F. Hwang, and J.M. Tour. .*J. Am. Chem. Soc.* **2008**, 130, 16201